Journal of Atmospheric and Solar-Terrestrial Physics 120 (2014) 70–79

Contents lists available at ScienceDirect

Journal of Atmospheric and Solar-Terrestrial Physics

journal homepage: www.elsevier.com/locate/jastp

A new South American network to study the atmospheric electric field and its variations related to geophysical phenomena

J. Tacza [a,*], J.-P. Raulin [a], E. Macotela [a], E. Norabuena [b], G. Fernandez [c], E. Correia [a,d], M.J. Rycroft [e], R.G. Harrison [f]

[a] Centro de Radio Astronomia e Astrofísica Mackenzie (CRAAM), Escola de Engenharia, Universidade Presbiteriana Mackenzie, São Paulo, SP, Brazil
[b] Instituto Geofísico del Perú, IGP, Lima, Peru
[c] Complejo Astronómico El Leoncito, CASLEO, San Juan, Argentina
[d] Instituto Nacional de Pesquisas Espaciais, Ministério da Ciência e Tecnologia, São José dos Campos, Brazil
[e] CAESAR Consultancy, 35 Millington Road, Cambridge CB3 9HW, UK
[f] Department of Meteorology, University of Reading, Earley Gate, Reading RG6 6BB, UK

ARTICLE INFO

Article history:
Received 14 May 2014
Received in revised form
1 September 2014
Accepted 2 September 2014
Available online 6 September 2014

Keywords:
Potential gradient
Carnegie curve
Global Atmospheric Electric Circuit
Temporal variations

ABSTRACT

In this paper we present the capability of a new network of field mill sensors to monitor the atmospheric electric field at various locations in South America; we also show some early results. The main objective of the new network is to obtain the characteristic Universal Time diurnal curve of the atmospheric electric field in fair weather, known as the Carnegie curve. The Carnegie curve is closely related to the current sources flowing in the Global Atmospheric Electric Circuit so that another goal is the study of this relationship on various time scales (transient/monthly/seasonal/annual). Also, by operating this new network, we may also study departures of the Carnegie curve from its long term average value related to various solar, geophysical and atmospheric phenomena such as the solar cycle, solar flares and energetic charged particles, galactic cosmic rays, seismic activity and specific meteorological events. We then expect to have a better understanding of the influence of these phenomena on the Global Atmospheric Electric Circuit and its time-varying behavior.

1. Introduction

The confirmation in 1753 (Parsons and Mazeas, 1753; Canton, 1753) that the atmospheric electric field recently identified in thunderstorm conditions persists in fair weather immediately raised questions of how it originates and by which mechanism (s) it is maintained. Here fair weather conditions means that no local electrification processes are occurring in the atmosphere, and the absence of appreciable convective clouds.

Investigations of fair weather electrification phenomena were performed during the late eighteenth and nineteenth centuries, but major advances came with measurements made by the Carnegie Institution of Washington in the early twentieth century. On board a ship, the vertical atmospheric electric field in the atmosphere was measured every hour in the oceanic air. Analysis of the results showed that the daily electric field variation with Universal Time was independent of the ship's position. This diurnal variation is a key part of our contemporary understanding of the Global Atmospheric Electric Circuit (GAEC), and is generally known as the Carnegie curve (Harrison, 2013). The Carnegie curve was obtained from the averaging of thousands of measurements of the Earth's fair weather electric field in terms of the Universal Time of the measurements over the world's oceans where the planetary boundary layer is relatively free of pollution. In fair weather, the vertical atmospheric electric field is about $E = -130$ V/m, where the minus sign indicates that the electric field vector is pointing downwards. Meteorologists refer to the potential gradient (PG) rather than the electric field (E). The PG and E have the same magnitude, although by convention the PG is positive in fair weather.

The GAEC is formed between the Earth's surface, which is a good conductor of electricity, and the ionosphere, a weakly ionized plasma at and above ~80 km altitude. Between these two layers the atmosphere is a reasonably good electrical insulator, i.e. it is a leaky dielectric medium. Electrical "batteries" exist below or inside electrified clouds (e.g., precipitation as rain or thunderclouds) to maintain the atmospheric electric field, implying that an electric current flows up to the ionosphere above these clouds. The electric circuit is closed by downward currents flowing through the fair weather and semi-fair weather regions of the Earth's atmosphere,

* Corresponding author. Fax: +55 11 32142300.
E-mail address: josect1986@gmail.com (J. Tacza).

http://dx.doi.org/10.1016/j.jastp.2014.09.001
1364-6826/

and through the rocks and oceans of the Earth's surface (Rycroft et al., 2008).

The well-known close correlation between the electrical generating system of the GAEC and the Carnegie curve has been mentioned by several authors (Rycroft et al., 2000, 2008; Williams, 2009; Harrison, 2013). However, the exact link is not well understood and continuous monitoring of the atmospheric electric field is required in different geographical areas to help in the interpretation of the behavior of the GAEC (Rycroft et al., 2012).

Solar and space weather phenomena affect the ionosphere causing disturbances in the GAEC (Rycroft et al., 2000, 2012), which can be monitored by analyzing the variations of the atmospheric electric field in fair weather. Transient variations of the intensity of the atmospheric electric field have also been systematically reported in association with time fluctuations of the secondary cosmic ray flux measured at the same location (De Mendonça et al., 2010). Such observations open up new possibilities for a better understanding of the relationship between extreme variations of the electrical properties of the atmosphere, such as during lightning, and Forbush effect decreases.

The GAEC has also been studied to look for short-term precursors of seismic activity. The main reason is that increased radon emanation and/or electrical charge generated by cracking rocks and associated in time and space with strong seismic events is nowadays an undisputed observational fact (see, for example, Ghosh et al. (2009) and Pulinets and Boyarchuk (2004)). Furthermore, the radon decay process dominates the amount of atmospheric ionization in the near-Earth boundary layer and, therefore, changes of radon concentration there will significantly affect the electrical conductivity, which in turn will produce changes on the measured atmospheric electric field (Pierce, 1976). However, these changes are difficult to observe because of the great variety of phenomena and perturbations that can affect its value, such as fog, strong winds, precipitation, aerosols, and pollution (Bennett and Harrison, 2007). Therefore, the search for earthquake precursor effects in the atmospheric PG (Harrison et al., 2010, 2014) needs the behavior of the atmospheric electric field in fair-weather conditions to be known for various meteorological variable conditions.

2. Scientific objectives of the network

In this section we describe the scientific motivations and objectives for the operation of a new atmospheric electric field monitoring network in the South American region.

2.1. Relationship between the Carnegie curve and the generators of the Global Atmospheric Electric Circuit

According to the classical picture of atmospheric electricity, the overall thunderstorm activity at any time charges the ionosphere to a positive potential of several hundred thousand volts with respect to the Earth's surface. This potential difference drives a vertical electric conduction current downward from the ionosphere to the ground in all fair-weather regions of the globe (Rycroft and Harrison, 2012; Rycroft et al., 2000). Horizontal currents flow freely within the highly conducting Earth's surface and in the ionosphere. A current flows upward from the top of thunderstorm clouds toward the ionosphere and also from the ground into the thunderstorm generator, closing the circuit (Rycroft et al., 2000). At first, thunderstorms were thought to be the only “batteries” that maintain the global electric circuit. This was shown in the study of Whipple (1929) which compared the Carnegie curve with variations of the world's thunderstorm areas. However, these two differ quantitatively in two key aspects: a) the relative amplitude variation of the thunderstorm areas over land is more than twice that of the Carnegie curve, and b) the time of maximum global thunderstorm activity corresponds to afternoon local times in Africa, whereas the Carnegie curve maximizes for afternoon local times in South America (Liu et al., 2010).

In order to try to understand these discrepancies, Kartalev et al. (2006) used a theoretical model to estimate the effects of upward currents from a thunderstorm to the ionosphere. They showed that the Carnegie curve preferentially reflects the longitudinal distribution of thunderstorms within 11° magnetic latitude of the magnetic dip equator. South American thunderstorms are close to the magnetic dip equator, whereas most African thunderstorms occur over the Congo at a more southerly dip latitude between 12° and 20°. Thus, South American thunderstorm sources seem to have a greater influence on the Carnegie curve than the more numerous thunderstorm sources over Africa.

In a more recent study, Liu et al. (2010) compared the Carnegie curve with the Universal Time diurnal variations of rainfall from thunderstorms and electrified shower clouds (ESCs) using a 10-year database from the Tropical Rainfall Measuring Mission (TRMM). These authors concluded that not only do thunderstorms contribute to the Carnegie curve, but rainfall outside thunderstorm regions is also important. The same conclusions were reached for fair weather electric field measurements made in Vostok, Antarctica, performed by Burns et al. (2005). Blakeslee et al. (2014) using data obtained from the Optical Transient Detector (OTD) and the Lightning Imaging Sensor (LIS) satellites, complemented with other electrical observations from high altitude aircraft missions, found that the total global current is distributed as follows: Land thunderstorms (52%), ocean thunderstorms (31%), non-lightning producing ocean ESCs (15%) and land ESCs (2%). These findings are consistent with predictions by Wilson (1903) that negative charge is carried down by rain (precipitation) and that this current generator plays a part in maintaining the global electrical circuit. Similarly, Wilson (1920) speculated that both thunderstorms and electrified shower clouds account for the descent of negative charge. Despite Africa's dominance in lightning occurrence, its contribution to the diurnal variation of the global circuit is less important than that of the Americas because of the larger electrified rainfall contribution from this region.

It is now known that the Global Atmospheric Electric Circuit, driven by thunderstorms and electrified rain/shower clouds, is also influenced by energetic charged particles from space (Rycroft et al., 2012). However, more observational studies in different geographical regions are needed to investigate this in detail. For this reason, one of the objectives of the new network is to provide reliable electrical field time profiles in fair weather conditions to help obtain a better understanding of the behavior of the GAEC.

2.2. Solar-terrestrial effects

Solar activity varies over a cycle with a period of ~11 years. The solar magnetic field and its extension through the interplanetary medium up to the Earth's orbit and beyond is much more variable at solar maximum than at solar minimum. The flux of galactic cosmic rays and the flux of energetic charged particles from the Sun are also subject to this variation. These energetic charged particles as well as those precipitating from the magnetospheric radiation belts during geomagnetic disturbances interact with the Earth's middle and lower atmosphere. They deposit their energy by ionization, by modifying atmospheric chemistry, or by affecting the nucleation of water droplets to form clouds (Rycroft et al., 2000). For these reasons the solar cycle plays an important role in the variations of the GAEC. In addition to long-term changes (i.e. solar cycle variations), the global electric circuit is also affected by short-term solar variations, such as solar flares and solar magnetic

sector boundary crossings in interplanetary space. A summary of how the global electric circuit is affected by long-and short-term solar variations can be found in Rycroft et al. (2012). Although there is some evidence for a solar influence on atmospheric electrical parameters, the solar-terrestrial electrical coupling mechanisms are not well understood (Rycroft et al., 2012).

2.3. Cosmic rays

The fluxes of galactic and solar cosmic rays entering the Earth's atmosphere are essential to the GAEC, since these charged particles are the main source of atmospheric ionization at about 15 to 20 km altitude, and above (Rycroft et al., 2012). The propagation through the atmosphere of secondary cosmic rays can in principle be affected by the presence of electric fields (Muraki et al., 2004; De Mendonça, 2011).

Markson (1981) found positive correlations between variations of the cosmic radiation measured on the ground, and changes of the ionospheric potential derived from aircraft and balloon measurements. Ground measurements show cosmic ray flux excesses in the presence of electric fields associated with thunderclouds (Muraki et al., 2004; De Mendonça et al., 2009; Raulin et al., 2014). Moreover, recently Toropov et al. (2013) found that neutron bursts can be produced in association with negative lightning discharges. These results indicate that cosmic ray showers in the atmosphere may play an important role in the physical processes responsible for cloud formation and lightning discharges.

Data from the new network should lead to a better understanding of the relation between changes in the electrical properties of the atmosphere and measured changes in the simultaneously observed cosmic ray fluxes.

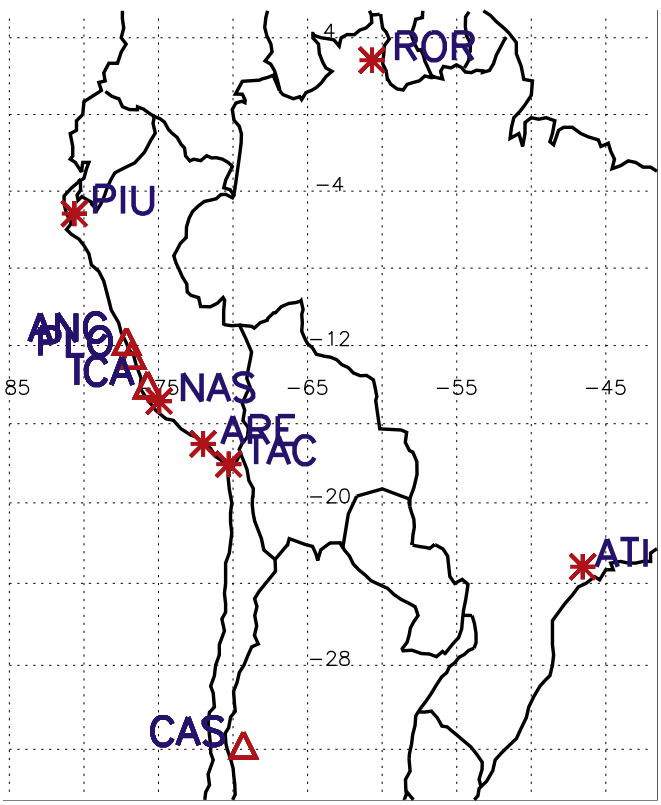

Fig. 1. EFM sensors already installed (triangles), and future locations for new sensors (stars).

2.4. Atmospheric electric field and seismic activity

The variation of the atmospheric electric field in fair-weather has been analyzed to look for short-term precursors of seismic activity. One of the main reasons for this is the close association between the emanation of radon gas and the occurrence of seismic activity (see the review by Ghosh et al. (2009)). The relationship between radon emanation and the atmospheric electric field has been studied qualitatively by Pierce (1976) who indicated that the release of radon from the ground may increase substantially before an earthquake, causing a decrease in the atmospheric electric field in fair-weather. Recent studies (Harrison et al., 2014) have proposed a mechanism for modeling ionospheric disturbances, by considering Atmospheric Lithosphere-Ionosphere Charge Exchange (ALICE) processes during radon gas emanations (see, for example, Pulinets and Boyarchuk (2004) and Harrison et al. (2010)). These effects are evidenced quantitatively in Hao et al. (1998) and Silva et al. (2012). Finally, Mikhailov et al. (2004) reported variations of the fair-weather atmospheric electric field power spectrum before an earthquake. For these reasons, the new network has been strategically installed in highly seismic areas, one of its objectives being the search for atmospheric electric field anomalies prior to seismic events.

2.5. Meteorological variations

Atmospheric electricity and its relationship with meteorological phenomena have been studied since the eighteenth century. Lord Kelvin at this time had no doubt that the study of atmospheric electrical indicators would bring important clues to increase our knowledge of weather forecasting (Thomson, 1872). Observations confirm that weather changes (fog, wind direction, rain, hail, sleet, snow, etc.) are often associated with pronounced changes of the mean atmospheric electric field values in fair weather (Dolezalek, 1963; Nizamuddin and Ramanadham, 1983; Bennett and Harrison, 2007).

Thus, one of the objectives of the new network is to collect data and to continue the study of fair-weather atmospheric electric field measurements associated with the variations of meteorological parameters. Therefore, in principle, one should be able to

Table 1
Description of existing sensors EFM stations, installed in South America.

Location	Latitude (deg)	Longitude (deg)	Height (m)	Description
CAS1	−31. 799	−69.297	2480	Installation in 01/2008. The sensor is located away of housing, surrounded scrub and low bushes in a mountainous region and away from industrial areas.
CAS2	−31. 800	−69.293	2480	Installation in 01/2010. Similar characteristics to CAS1.
ICA	−14.089	−75.736	402	Installation in 12/2011. The sensor is located in the center of the city of Ica away of housing. Some trees at a distance of 20 m.
PLO	−12.504	−76.798	85	Installation in 11/2011. The sensor is placed on the roof of housing, about 220 m away from the sea and 1700 m from the nearest town. No presence of nearby vegetation.
ANC	−11.777	−77.151	51	Installation in 10/2012. The sensor is placed on the roof of housing, about 1000 m of a highway and 1200 m from the nearest town, and about 2500 m away from the sea. Few trees at a distance of 40 m.

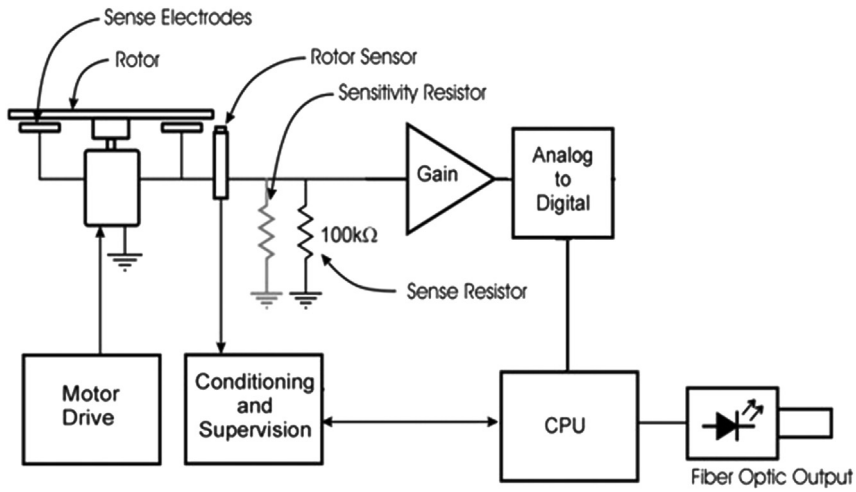

Fig. 2. Block diagram for EFM sensor (from Boltek Corporation EFM100-1000120-050205).

Fig. 3. Final position of the EFM sensor installed at El Leoncito (Argentina).

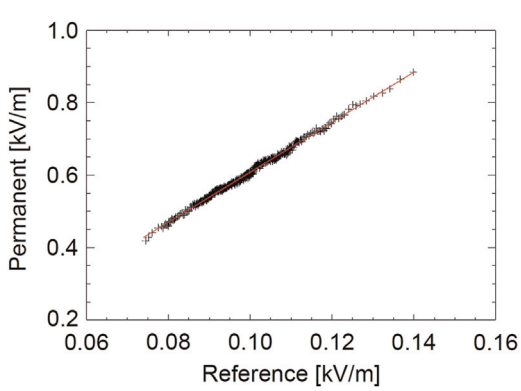

Fig. 4. Linear regression of EFM measurements, obtained at El Leoncito (Argentina), at ground level (Reference) and at the permanent final position (Permanent). Then, the values are corrected as follows: E permanent$=mE$ reference$+c$, where $m=7.36$ and $c=-0.09$ kV/m.

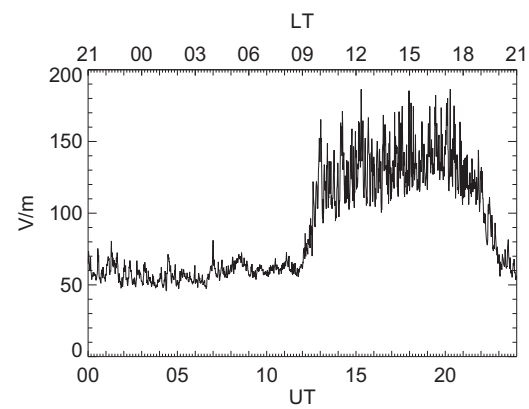

Fig. 5. Diurnal variation of the atmospheric electric field in fair-weather on 31 August, 2011.

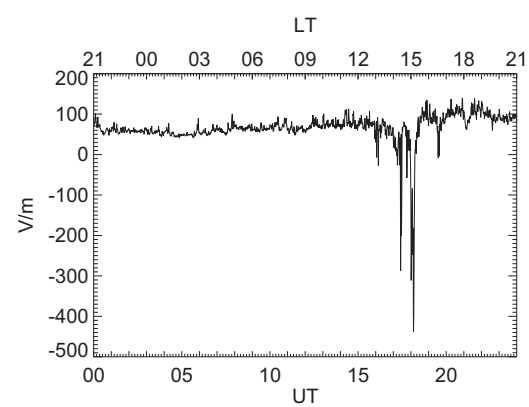

Fig. 6. Diurnal variation of atmospheric electric field in disturbed-weather on 26 August, 2011.

infer whether the electric parameters are only passive symptoms or active partners in these atmospheric processes.

3. Installation of the new network, data processing and first results

Continuous measurements of the atmospheric electric field are being recorded at various locations in South America. The already

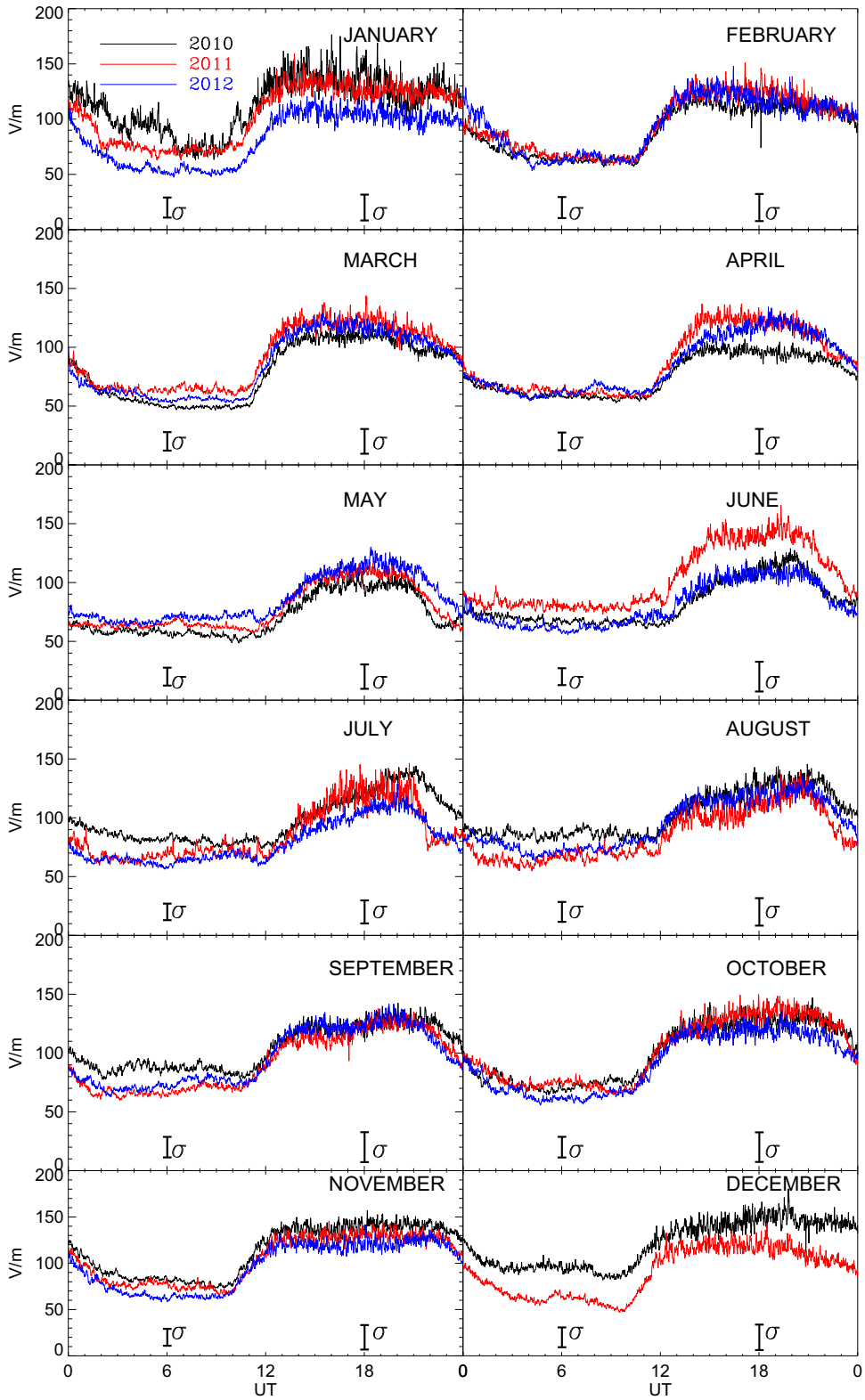

Fig. 7. Monthly variations of the atmospheric electric field at CAS station for three years (2010: black, 2011: red, 2012: blue). The error bars represent 1σ mean values for the three years in the night time (left) and day time (right). (For interpretation of the references to color in this figure legend, the reader is referred to the web version of this article.)

existing locations CAS (2 sensors named CAS1 and CAS2 at El Leoncito, San Juan, Argentina), ANC (1 sensor Ancon, Lima, Peru), PLO (1 sensor Punta Lobos, Lima, Peru) and ICA (1 sensor Ica, Peru) are shown by triangles in Fig. 1. New locations for sensor operation in 2014 are indicated in Fig. 1 by star symbols. A brief description of the stations is indicated in Table 1.

Each sensor consists of a commercially manufactured (Boltek Corporation EFM100-1000120-050205) electric field mill (EFM).

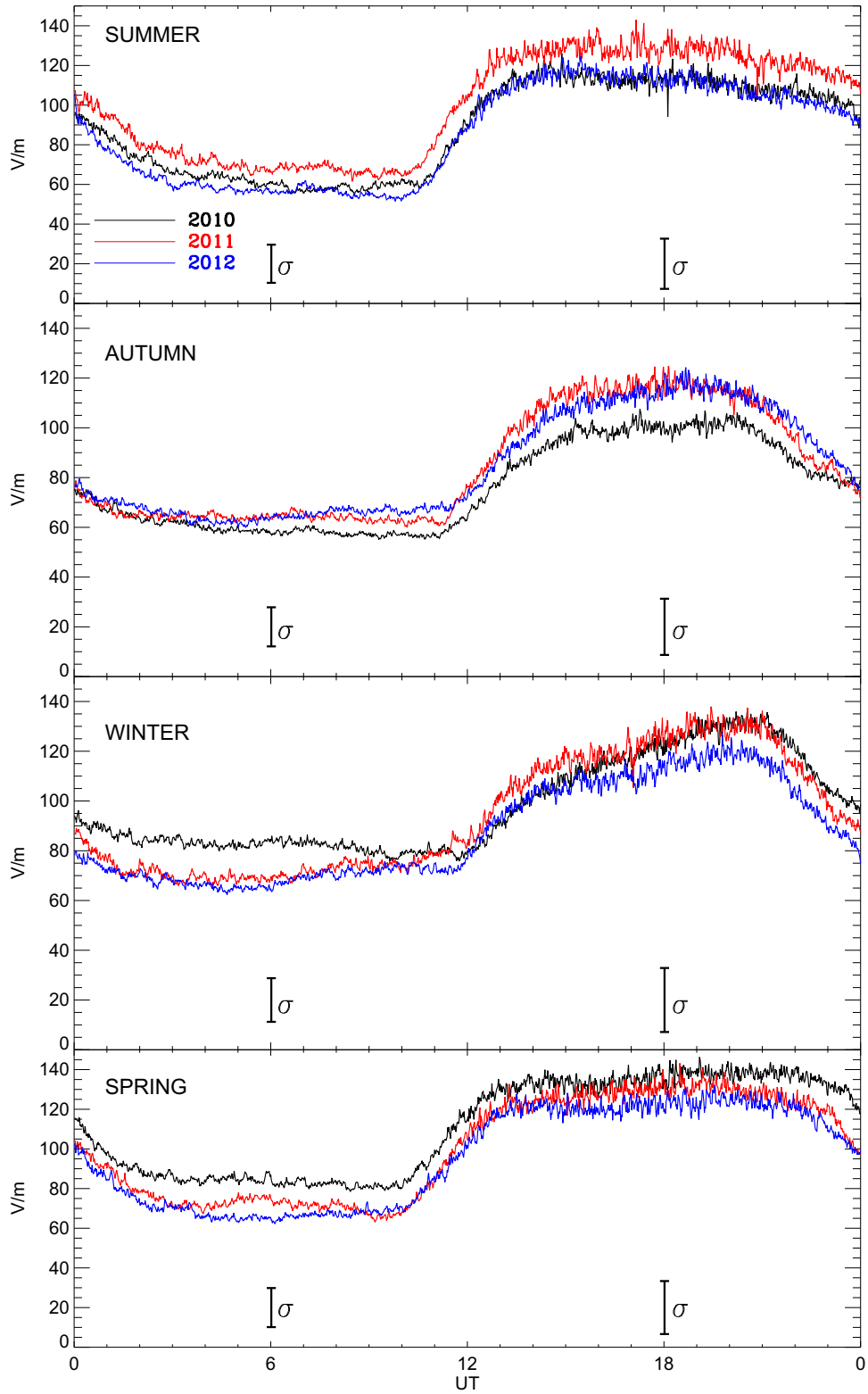

Fig. 8. As in Fig. 7, only that for seasonal variations.

Fig. 2 shows the basic principles of the EFM operation. A current flows from ground through the 100 kΩ resistor when the sensing electrode is exposed to the atmospheric electric field. When the sensing electrode is shielded from the influence of the electric field, the current flows to ground through the same resistor. The electrical potential drop through the resistor is then proportional to the intensity of the atmospheric electric field. A second resistor in parallel allows the sensitivity of the measurement to be changed in order to avoid saturation due to high electric field intensities, typically >20 kV/m, during stormy or lightning periods.

For actual readings of the atmospheric electric field, the EFM needs to be positioned at ground level. However, this is impractical because the presence of insects, animals, dirt and water can

damage the sensor. For this reason the EFM meter is placed at a certain height above the surface. For example, Fig. 3 illustrates the final position of the EFM sensor located at El Leoncito, at 0.8 m above the ground. However, electric field measurements performed above the ground are abnormally large. This effect is due to an increase of the density of electric field lines and electric charges at a raised conductor. To remove this effect, simultaneous observations have been made with two EFM sensors, named REF and PER. REF and PER are located at ground level and at the final permanent position, respectively. The linear regression between REF and PER recorded data is then calculated, as shown in Fig. 4, and is used to correct daily measurements obtained by the PER sensor. The same treatment is carried out for all the other stations.

In the following, as an example illustrating the network's capability, we show data obtained at CAS2 station. Electric field measurements are collected with a time resolution of 0.5 s, and integrated into 1 min averages for the analysis reported here. The results are summarized in Figs. 5–9. A typical daily curve obtained in fair weather conditions is shown in Fig. 5. Fig. 6 shows the typical diurnal variations during a disturbed day, in this case due to the presence of lightning activity nearby. For comparison, in Figs. 5 and 6, we also show local and Universal Time (LT and UT) in the upper and lower axis, respectively. The methodology adopted in our analysis was to obtain monthly mean curves of the diurnal variations of the atmospheric electric field in fair weather. The criteria for choosing days of fair weather was to select days with potential gradient variations in the range of 40-200 V / m, such as illustrated in Fig. 5. The resulting monthly curves are shown in Fig. 7 for the three years of 2010, 2011 and 2012. The monthly average curves of diurnal variation in fair weather conditions will then be used to compare with daily curves affected by various phenomena mentioned in section 2. Following the same methodology we obtain seasonal and annual curves shown in Fig. 8 and Fig. 9, respectively. The number and proportion of fair weather days selected for the monthly and seasonal curves are summarized in Table 2 and Table 3, respectively. Table 4 shows the mean electrical field value for each hour for the corresponding months in the time period analyzed.

One σ bars are shown in Figs. 7–9, where σ is a mean value of the root mean square deviation obtained from the 3 years of data for 00–12 UT (left) and 12–24 UT (right). It is particularly interesting to note, of these figures, that the shape of the daily variation averaged during a given month, season or year repeats itself almost identically for the different years. Specific time structures of a few hours duration are clearly seen to have similar shapes from year to year.

A gross similarity exists between the annual hourly diurnal variations measured at CAS2 and the Carnegie curve (see, e.g., Fig. 6a from Harrison (2013)). This comparison is shown in Fig. 10, for the three years of 2010, 2011 and 2012. Error bars represent $196\sigma/\sqrt{N}$, where σ is the standard deviation and N is the total number of fair weather days considered. The linear correlation coefficients R are greater than $R=0.9$ for the three years. In this figure the amplitude values for CAS2 obtained at 2480 masl were multiplied by 1.3 to match the Carnegie curve. This is to account for the exponential decrease of the atmospheric electric field with increasing altitude (Rycroft et al., 2000). However, according to theoretical models, the ratio between Carnegie and CAS2 should be of the order of 2–2.5 rather than 1.3 (Rycroft et al., 2007). One possible explanation for this difference may be because the sensor at CAS2 is located on top of a small hill in a mountainous region, so that the lines of force of the electric field are focused towards the peak, causing an overestimation of the measured electric field values. Indeed, reports of electric field measurements performed at 3400 masl (Cobb, 1968) and 4300 masl (Xu et al., 2013) also show high mean values of 120 V/m and 163 V/m, respectively, higher than what they should at these altitudes.

Another difference when comparing CAS2 measurements and the Carnegie curve concerns the shape of the variation with Universal Time. A great similarity is observed for the time period 14–01 UT with common maxima amplitude around 19–20 UT. However, between 02 and 14 UT we clearly note a large difference. Daily curve measurements performed at land stations are generally different when compared to the Carnegie curve due to local phenomena, such as pollution and aerosols. Similarly, measurement performed at different stations do not show the same minimum and maximum times as in the Carnegie curve

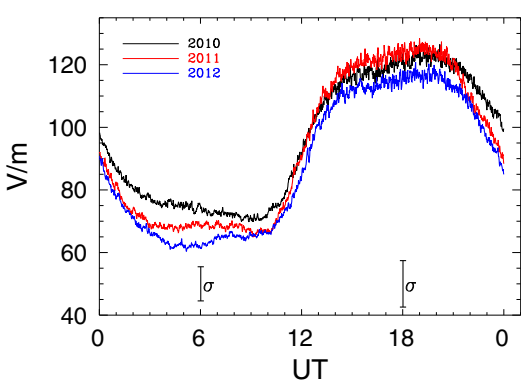

Fig. 9. As in Fig. 7, only that for annual variations.

Table 3
Total number and proportion of fair weather days selected at CAS station, by season.

Year/Season	Summer	Autumn	Winter	Spring	Total
2010	32	51	38	42	163
Proportion	20%	31%	23%	26%	100%
2011	26	48	30	37	141
Proportion	19%	34%	21%	26%	100%
2012	32	53	39	40	164
Proportion	20%	32%	24%	24%	100%

Table 2
Total number and proportion of fair weather days selected at CAS station, by month.

Year/Month	Jan	Feb	Mar	Apr	May	June	July	Aug	Sept	Oct	Nov	Dec	Total
2010	3	17	19	20	13	15	18	10	13	10	18	10	166
Proportion	2%	10%	11%	12%	8%	9%	11%	6%	8%	6%	11%	6%	100%
2011	9	8	14	16	21	10	4	5	18	12	16	8	141
Proportion	6%	6%	10%	11%	15%	7%	3%	4%	13%	8%	11%	6%	100%
2012	8	6	21	18	21	8	15	12	20	17	15	0	161
Proportion	5%	4%	13%	11%	13%	5%	9%	8%	12%	11%	9%	0%	100%

Table 4
The mean electrical field value (in V/m) for each hour for the corresponding months for the three years.

Hour (UT)	January			February			March			April			May			June		
	2010	2011	2012	2010	2011	2012	2010	2011	2012	2010	2011	2012	2010	2011	2012	2010	2011	2012
1	124	109	91	89	92	109	83	83	75	71	76	74	64	64	73	74	86	75
2	115	94	74	78	86	96	68	70	65	66	68	69	60	64	71	73	82	68
3	104	77	64	71	83	78	60	65	64	64	64	64	57	63	67	71	83	64
4	93	77	57	67	74	67	56	64	62	60	63	60	60	64	66	69	82	63
5	97	74	56	66	72	59	54	62	59	58	65	58	57	63	66	69	81	62
6	94	70	53	63	66	61	50	64	55	59	63	60	59	64	68	67	81	61
7	80	70	53	63	66	65	49	65	55	58	62	61	56	68	72	67	79	58
8	72	72	55	62	65	67	49	66	57	58	61	65	58	64	70	66	79	63
9	75	71	51	62	63	64	49	64	56	57	61	67	55	63	70	66	78	61
10	77	73	53	64	63	63	49	63	55	56	59	64	54	62	72	67	79	65
11	98	81	60	63	65	66	50	63	56	57	59	61	53	61	73	66	83	70
12	117	107	77	83	88	89	64	80	72	61	65	66	56	61	70	64	87	72
13	133	123	98	104	110	109	88	105	97	76	87	79	63	70	76	68	93	73
14	140	131	106	114	120	121	102	119	110	90	107	94	76	86	87	81	114	88
15	143	133	109	117	125	125	108	122	117	97	122	106	86	97	101	91	130	97
16	138	133	107	114	127	127	109	124	121	98	124	109	97	104	108	100	139	103
17	138	128	105	111	125	124	108	120	118	97	125	113	97	106	111	104	138	104
18	137	128	106	111	125	120	109	123	118	98	124	117	101	109	113	107	138	108
19	137	124	106	112	128	116	110	125	115	96	122	121	96	110	119	114	140	108
20	125	128	103	113	122	116	108	120	114	94	121	122	99	107	116	117	146	106
21	117	125	102	111	118	109	104	114	109	95	116	115	98	105	112	116	140	109
22	123	124	98	113	112	113	97	111	106	91	110	112	85	91	107	101	127	99
23	131	124	101	109	108	111	96	106	100	88	94	102	65	75	91	86	112	83
24	121	119	98	101	105	104	93	96	91	79	89	88	66	65	79	83	93	76
Hour (UT)	July			August			September			October			November			December		
	2010	2011	2012	2010	2011	2012	2010	2011	2012	2010	2011	2012	2010	2011	2012	2010	2011	2012
1	96	79	71	89	74	84	97	80	81	88	94	88	114	105	98	114	91	-
2	90	68	63	86	64	80	88	66	75	78	86	75	99	89	83	100	79	-
3	87	67	66	86	64	78	82	67	67	79	76	68	90	79	73	96	68	-
4	84	64	64	85	60	72	88	65	70	71	72	67	84	76	67	94	62	-
5	81	65	62	84	61	68	91	65	69	70	72	60	83	78	66	97	59	-
6	81	68	59	85	66	70	87	65	72	68	75	61	84	79	62	98	65	-
7	83	68	62	86	67	73	87	67	73	70	75	61	82	74	64	95	63	-
8	80	72	65	90	66	74	88	70	78	73	73	61	79	74	64	95	60	-
9	80	72	66	86	71	73	88	73	79	76	70	64	76	73	64	86	55	-
10	77	75	69	85	68	77	84	71	77	76	68	67	76	69	66	87	50	-
11	80	71	69	84	73	81	81	71	74	79	73	71	92	82	83	100	65	-
12	79	69	63	84	71	83	89	83	81	96	95	86	116	104	101	119	93	-
13	80	72	70	97	88	99	106	97	101	112	111	105	131	121	117	132	110	-
14	90	85	79	109	100	110	114	109	117	120	121	117	138	126	120	137	116	-
15	100	101	88	114	101	116	122	113	121	123	124	117	137	128	121	138	119	-
16	107	108	94	118	101	115	122	111	124	124	128	117	135	128	117	141	120	-
17	115	120	98	120	102	116	121	113	122	124	133	118	138	129	117	142	120	-
18	119	122	102	127	110	117	122	119	121	128	134	120	140	131	120	149	119	-
19	124	119	109	128	113	121	125	126	126	127	135	119	143	132	122	151	120	-
20	133	120	111	131	118	122	129	126	131	127	138	122	142	132	119	154	119	-
21	137	123	111	131	125	125	129	126	128	130	135	119	141	129	124	145	110	-
22	133	101	100	133	115	121	128	124	121	131	132	115	142	129	126	143	106	-
23	117	80	85	119	93	109	124	114	107	122	124	109	139	128	124	145	102	-
24	106	84	79	106	78	93	112	98	92	112	107	99	131	116	111	142	96	-

(Yeboah-Amankwah, 1989; Kamra et al., 1994; Harrison, 2003; Kumar et al., 2009; Guha et al., 2010; De et al., 2013). Nevertheless, in some cases good correlations have been found (Israelsson and Tammet, 2001; Harrison, 2003; Marcz and Harrison, 2003). A possible explanation for the difference found in our results at CAS2 stations, is that measurements are dominated by the effects of tropical convective clouds (Hendon and Woodberry, 1993) and the large lightning rate in South America (Blakeslee et al., 2014). In this case CAS2 measurements show a regional effect rather than a global one. Another possibility would be that the Asian lightning peak occurrence, generally observed in the Carnegie curve around 6–9 UT and assumed to be part of the generator system of the GAEC, does not contribute much to the CAS2 measurements due to attenuation because of the large distance. Indeed, measurements performed over the Indian Ocean show a tendency for higher effects of storm activity over Asia–Australia and Africa–Europe and lower effects of far distant storms over America (Kamra et al., 1994).

Although we have indicated several reasons why our measurements may differ from the Carnegie curves, as indeed other do, to identify the mechanisms for these discrepancies is beyond the scope of this paper and will be studied elsewhere. More important is that we will be able to identify the signatures of possible drivers (see Section 2) in daily time integrated atmospheric electric field variations, if they are enough intense. Therefore, a simple difference between the records obtained during disturbed conditions and the monthly fair weather average, both measured at the same location, will allow isolating the signature of these possible drivers. This should be the procedure in the future, irrespective of whether the average fair weather curves do resemble the Carnegie curve or not, which is a separate research question.

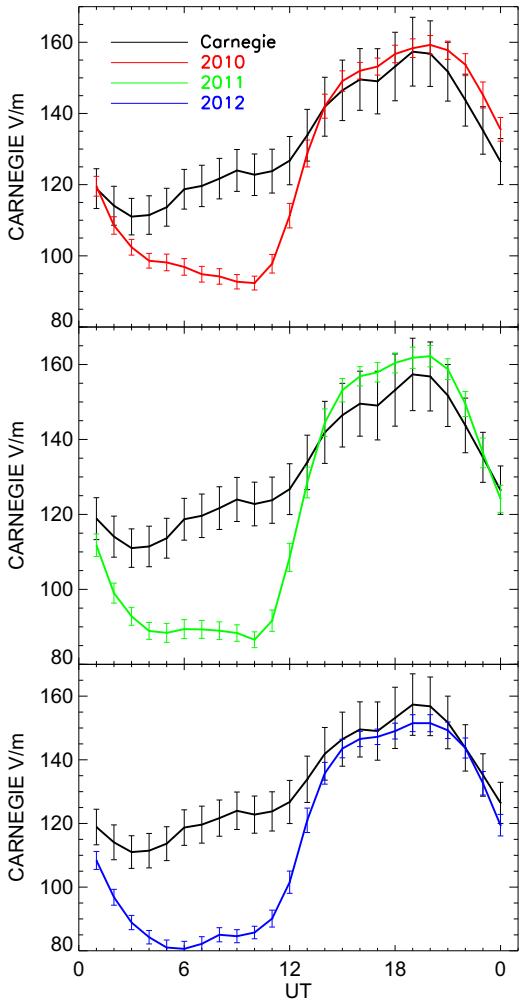

Fig. 10. Annual hourly variations of the atmospheric electric field at CAS station for three years (2010: red, 2011: green, 2012: blue), compared with the Carnegie curve (black). The error bars represent the range of 1.96 standard errors on the mean, corresponding to a 95% confidence interval on the mean. The linear correlation coefficient r between the 24 hourly data values of electric field in CAS and Carnegie are $r=0.91$ (2010), 0.95 (2011) and 0.94 (2012). (For interpretation of the references to color in this figure legend, the reader is referred to the web version of this article.)

4. Conclusions

In this paper we have discussed a new instrumental facility in South America consisting of a network of electric field mills to monitor the vertical atmospheric electric field close to the Earth's surface. Composed of five stations at the present time, we plan to have a few more instruments installed in 2014 which is one the main advantages of this new undertaking in the field of atmospheric electricity. The preliminary results shown here indicate the possibility of providing reliable diurnal variation curves, in all seasons, of the fair weather atmospheric electric field. These curves closely resemble the classical daily variation apparent in the Carnegie curve. Such results will be important to assess how the properties of the GAEC vary as a function of time on different scales. The departures from fair weather diurnal variations will then be used to study the behavior of the GAEC in relation to solar and space weather phenomena and to variations of the galactic cosmic ray flux. We shall also look for short-term atmospheric electricity precursors of enhanced seismic activity in the region, and analyze the observations with respect to local meteorological parameters.

Acknowledgments

JPR, EM and JT thank the CNPq funding agency (Proc. 305655/2010-8, 482000/2011-2, 130082/2013-9 and 130083/2013-5). Authors are grateful to two anonymous reviewers for their constructive comments and suggestions, which helped to improve the quality of the paper.

References

Bennett, A.J., Harrison, R.G., 2007. Atmospheric electricity in different weather conditions. Weather 62 (10), 277–283.
Blakeslee, R.J., Mach, D.M., Bateman, M.G., Bailey, J.C., 2014. Seasonal variations in the lightning diurnal cycle and implication for the global electrical circuit. Atmos. Res. 135–136, 228–243.
Burns, G.B., Frank-Kamenetsky, A.V., Troshichev, O.A., et al., 2005. Interannual consistency of bimonthly differences in diurnal variations of the ground-level, vertical electric field. J. Geophys. Res. 110, D10106. http://dx.doi.org/10.1029/2004JD005469.
Canton, J., 1753. Electrical experiments, with an attempt to account for their several phenomena; together with some observations on thunder-clouds. Philos. Trans. R. Soc. Lond. 48 (1753–1754), 350–358.
Cobb, W., 1968. The atmospheric electric climate at Mauna Loa Observatory, Hawaii. J. Atmos. Sci. 25, 470–480.
De, S.S., Paul, S., Barui, S., et al., 2013. Studies on the seasonal variation of atmospheric electricity parameters at a tropical station in Kolkata, India. J. Atmos. Sol.-Terr. Phys. 105–106, 135–141. http://dx.doi.org/10.1016/j.jastp.2013.09.006.
De Mendonça, R.R.S., Raulin, J.-P., et al., 2009. Observation of cosmic ray and electric field variations in the surface atmosphere. Bull. Russ. Acad. Sci.: Phys. 73 (3), 1410–1416.
De Mendonça, R.R.S., Raulin, J.-P., Bertoni, F.C.P., et al., 2010. Long-term and transient time variation of cosmic ray fluxes detected in Argentina by CARPET cosmic ray detector. J. Atmos. Sol.-Terr. Phys. , http://dx.doi.org/10.1016/j.jastp.2012.09.034.
De Mendonça, R.R.S., 2011. Influência das variabilidades solar, geomagnética e atmosférica na modulação da intensidade de raios cósmicos. INPE, São Jose dos Campos, SP, Brazil (Master's thesis).
Dolezalek, H., 1963. The atmospheric electric fog effect. Rev. Geophys. 1, 231–282.
Ghosh, D., Deb, A., Sengupta, R., 2009. Anomalous radon emission as precursor of earthquake. J. Appl. Geophys. 69, 67–81.
Guha, A., De, B.K., Gurubaran, S., et al., 2010. First results of fair-weather atmospheric electricity measurements in Northeast India. J. Earth Syst. Sci. 119 (2), 221–228.
Hao, J.-G., Tang, T.-M., Li, D.-R., 1998. A kind of information on short-term and imminent earthquake precursors-Research on atmospheric electric field anomalies before earthquakes. Acta Seismol. Sin. 11 (1), 121–131.
Harrison, R.G., 2003. Twentieth-century atmospheric electrical measurements at the observatories of Kew, Eskdalemuir and Lerwick. Weather 58, 11–19. http://dx.doi.org/10.1256/wea.239.01.
Harrison, R.G., 2013. The Carnegie Curve. Surv. Geophys. 34 (2), 209–232. http://dx.doi.org/10.1007/s10712-012-9210-2.
Harrison, R.G., Aplin, K.L., Rycroft, M.J., 2010. Atmospheric electricity coupling between earthquake regions and the ionosphere. J. Atmos. Sol.-Terr. Phys. 72, 376–381.
Harrison, R.G., Aplin, K.L., Rycroft, M.J., 2014. Brief communication: earthquake-cloud coupling through the global atmospheric electric circuit. Nat. Hazards Earth Syst. Sci. 14, 773–777. http://dx.doi.org/10.5194/nhess-14-773-2014.
Hendon, H.H., Woodberry, K., The diurnal cycle of tropical convection. J. Geophys. Res., 98, 1993, (D9), 16623-16637.
Israelsson, S., Tammet, H., 2001. Variation of fair weather atmospheric electricity at Marsta Observatory, Sweden, 1993–1998. J. Atmos. Sol.-Terr. Phys. 63, 1693–1703.
Kamra, A.K., Deshpande, C.G., Gopalakrishnan, V., 1994. Challenge to the assumption of the unitary diurnal variation of the atmospheric electric field based on observations in the Indian Ocean, Bay of Bengal and Arabian Sea. J. Geophys. Res. 99 (D10), 21,043–21,050.
Kartalev, M.D., Rycroft, M.J., Fuellekrug, et al., 2006. A possible explanation for the dominant effect of South American thunderstorms on the Carnegie curve. J. Atmos. Sol.-Terr. Phys. 68, 457–468.
Kumar, V.V., Ramachandran, V., Buadromo, V., et al., 2009. Surface fair-weather potential gradient measurements from a small tropical island station Suva, Fiji. Earth Planets Space 61, 747–753.
Liu, C., Williams, E., Zipser, E.J., Burns, G., 2010. Diurnal variations of global thunderstorms and electrified shower clouds and their contribution to the global electrical circuit. J. Atmos. Sci. 67, 309–323. http://dx.doi.org/10.1175/2009JAS3248.1.
Marcz, F., Harrison, R.G., 2003. Long-term changes in atmospheric electrical parameters observed at Nagycenk (Hungary) and the UK observatories at Eskdalemuir and Kew. Ann. Geophys. 21, 2193–2200. http://dx.doi.org/10.5194/angeo-21-2193-2003.

Markson, R., 1981. Modulation of the Earth's electric field by cosmic radiation. Nature 391 (5813), 304–308.
Mikhailov, Y.M., Mikhailova, G.A., et al., 2004. Power spectrum feature of the near-Earth atmospheric electric field in Kamchatka. Ann. Geophys. 47 (1), 237–245.
Muraki, Y., et al., 2004. Effects of atmospheric electric fields on cosmic rays. Phys. Rev. D 69, 123010.
Nizamuddin, S., Ramanadham, R., 1983. The electrical potential gradient in mist, haze and fog. Pure Appl. Geophys. 121, 353–359.
Parsons, J., Mazeas, W., 1753. Observations upon the Electricity of the Air, Made at the Chateau de Maintenon, during the Months of June, July, and October, 1753. Philos. Trans. R. Soc. Lond. 48 (1753–1754), 377–384.
Pierce, E.T., 1976. Atmospheric electricity and earthquake prediction. Geophys. Res. Lett. 3 (3), 185–188.
Pulinets S. and Boyarchuk K., Ionospheric Precursors of Earthquakes, 2004, Springer Verlag Publ. ISBN3-540-20839-9.
Raulin, J.-P., Tacza, J., Macotela, E., 2014. A new South America electric field monitor network. Sun Geosphere 9 (1–2), 111–114.
Rycroft, M.J., Israelsson, S., Price, C., 2000. The global atmospheric electric circuit, solar activity and climate change. J. Atmos. Sol.-Terr. Phys. 62, 1563–1576.
Rycroft, M.J., Odzimek, A., Arnold, N.F., et al., 2007. New model simulations of the global atmospheric electrical circuit driven by thunderstorm and electrified shower clouds: The roles of lightning and sprites. J. Atmos. Sol.-Terr. Phys. 69, 2485–2509.
Rycroft, M.J., Harrison, R.G., Nicoll, K.A., Mareev, E.A., 2008. An overview of Earth's global electric circuit and atmospheric conductivity. Space Sci. Rev. 137 (1–4), 83–105. http://dx.doi.org/10.1007/s11214-008-9368-6 (ISSN 0038-6308).
Rycroft, M.J., Harrison, R.G., 2012. Electromagnetic atmosphere-plasma coupling: the global atmospheric electric circuit. Space Sci. Rev. 168 (1–4), 363–384.
Rycroft, M.J., Nicoll, K.A., Aplin, K.L., Harrison, R.G., 2012. Recent advances in global electric circuit coupling between the space environment and the troposphere. J. Atmos. Sol.-Terr. Phys. 90-91, 198–211.
Silva, H.G., Oliveira, M.M., Serrano, C., et al., 2012. Influence of seismic activity on the atmospheric electric field in Lisbon (Portugal) from 1955 to 1991. Ann. Geophys. 55 (1), 193–197. http://dx.doi.org/10.4401/ag-5361.
Thomson, W., 1872. Reprint of Papers on Electrostatics and Magnetism (Section XVI, Atmospheric Electricity). Macmillan, London.
Toropov, A.A., Kozlov, V.I., et al., 2013. Experimental observations of strengthening the neutron flux during negative lightning discharges of thunderclouds with tripolar configuration. J. Atmos. Sol.-Terr. Phys. 94, 13–18.
Williams, E.R., 2009. The global electrical circuit: a review. Atmos. Res. 91, 140–152. http://dx.doi.org/10.1016/j.atmosres.2008.05.018.
Whipple, F.J.W., 1929. On the association of the diurnal variation of electric potential gradient in fine weather with the distribution of thunderstorms over the globe. Q. J. R. Meteorol. Soc. 55, 1–17.
Wilson, C.T.R., 1903. Atmospheric electricity. Nature 68, 101–104.
Wilson, C.T.R., 1920. Investigations on lightning discharges and on the electric field of thunderstorms. Philos. Trans. Roy. Soc. Lond. 221A, 73–115.
Xu, B., Zou, D., Chen, B., et al., 2013. Periodic variations of atmospheric electric field on fair weather conditions at YBJ, Tibet. J. Atmos. Sol.-Terr. Phys. 97, 85–90. http://dx.doi.org/10.1016/j.jastp.2013.02.013.
Yeboah-Amankwah, D., 1989. Fair weather electric field in Port Moresby. J. Atmos. Terr. Phys. 51, 1035–1040.